Spray-printed magnetoelectric multifunctional composites

P. Martins[1,2], J. S. Nunes[1,3], J. Oliveira[1,3], N, Peřinka[4] and S. Lanceros-Mendez[4,5]

[1]Centro de Física, Universidade do Minho, Braga, Portugal

[2]IB-S Institute of Science and Innovation for Sustainability, Universidade do Minho, 4710-057, Braga, Portugal

[3]Centro Algoritmi, Universidade do Minho, Guimarães, Portugal

[4]BCMaterials, Basque Centre for Materials, Applications and Nanostructures, UPV/EHU Science Park, 48940 Leioa, Spain.

[5]IKERBASQUE, Basque Foundation for Science, 48013-Bilbao, Spain

The performance of spray printed magnetoelectric (ME) composites based on poly(vinylidene fluoride-co-trifluoroethylene)/cobalt ferrite, P(VDF-TrFE)/$CoFe_2O_4$ is reported and discussed. It is shown that for a 20 wt.% ferrite content the composite exhibits a fibrillar-porous structure, ≈1.8 GPa Young's Modulus, saturation magnetization of 11.2 $emu.g^{-1}$, 6.0 $emu.g^{-1}$ magnetic remanence and a magnetic coercivity of 2050 Oe. Further, it is demonstrated a 34 dielectric constant (at 10 kHz) and a 27 $pC.N^{-1}$ piezoelectric coefficient. Such high dielectric and piezoelectric responses explain the ME response of 21.2 $mV{\cdot}cm^{-1}{\cdot}Oe^{-1}$ at an optimum magnetic field of 2450 Oe , which is superior to the response of similar composites prepared by bar-coating. The high ME response and the simple and scalable printing method demonstrates the suitability of these materials for cost effective and large-scale sensor/actuator applications.

1. Introduction

Additive manufacturing is rapidly expanding and modifying the way in which products are designed, optimized, manufactured and integrated[1]. With the possibility to transform digital information into physical components, this technology is leading to new routes in the manufacturing industry by producing complex geometries with tailored material properties, freedom on the design and environmental benefits, by transforming pre-defined files into fully functional products[2].

In this scenario, printing technologies are becoming increasingly popular for the development of functional devices[3]. Particularly interesting is the development of smart materials compatible with printing technologies, such as shape-memory materials, electroactive and magnetoactive materials, [4].

Smart materials obtained through printing technologies are particularly suitable for the development and implementation of printed electronics field, a highly increasing research and technological field[4]. Despite several reports regarding the development of conductors, dielectric, and semiconductor inks for different electronic components, there are still few reports of fully-printed devices[3,4]. In particular, for an effective next generation of fully printed sensing devices and systems, it is required the development of functional inks based on smart materials, including magnetic, ferroelectric, piezoelectric and in some cases magnetoelectric[3-5].

Polymers offer several advantages for an effective printing of smart materials due to the higher versatility than inorganic materials, higher flexibility, suitability to be implemented in a variety of substrates, possibility of tailoring their side-chains and molecular structure, opportunity to introduce active (nqano)fillers, as well as particles with specific properties into the material, enabling materials to be fabricated with specific chemical and physical properties[4]. Despite this favourable context, many printing methods are very specific for a given application and only a few are applicable to a wide range of materials and surfaces[4]. An effective and simple solution-based method for the preparation of polymer-based smart composite films is spray printing due to its high production velocity, efficient use of materials, good reproducibility and compatibility with different substrates[6].

XX

In this context, this paper presents a poly(vinylidene fluoride-co-trifluoroethylene)/$CoFe_2O_4$-based ink, which is then printed in a glass substrate trough

spray-printing and fully characterized with respect to its functional response, including piezoelectric, magnetic and magnetoelectric responses.

Poly(vinylidene fluoride-co-trifluoroethylene) (P(VDF-TrFE)) was selected due to its high piezoelectric response ($|d_{33}|\approx 30$ pC.N^{-1}) at room temperature and physicochemical stability; while $CoFe_2O_4$ was selected due to its high magnetostrictive coefficients (λ=200 ppm), high Curie temperatures, chemical stability, wear resistanceand simple processability[7,8].

2. Experimental

2.1 Materials

$CoFe_2O_4$ nanoparticles (≈35-50nm) were purchased from Nanostructured & Amorphous Materials, Inc. (Texas, USA) . N,N-dimethylformamide (DMF), pure grade, was supplied by Fluka (New Jersey, USA) and P(VDF-TrFE) was supplied by Solvay (Brussels, Belgium). All the chemicals and particles were used as received from the suppliers.

2.2 Ink preparation and printing conditions

The composite solutions were prepared following the general guidelines presented in the protocol XXX for the development of piezoelectric PVDF composites. In short, in order to obtain a good dispersion of the $CoFe_2O_4$ particles within the P(VDF-TrFE) matrix, the desired amount of ferrite (20% in weight percentage – wt.%) was added to DMF (10 mL) and then placed in an ultrasound bath (ATU ATM 3LCD) during 8 h to avoid a magnetic agglomeration, then 2 g of P(VDF-TrFE) were subsequently added and a $CoFe_2O_4$/ P(VDF-TrFE)/DMF-based ink was obtained. Flexible films were obtained by spray-printing the $CoFe_2O_4$/ P(VDF-TrFE)/DMF ink, using a commercial airbrush (Ventus Titan Dual Action 0.25mm), at 10 cm of the glass substrate using a pressure of 3 psi. Solvent evaporation was performed inside an oven at controlled temperature of 210 °C for 10 minutes. It is to notice that the solvent evaporation temperature is above the melting temperature of the polymer, but that it crystallizes in the electroactive phase when cooled down to room temperature. Then, the films (≈50 μm thick) were removed from the oven and allowed to cool at room temperature.

2.3 Sample characterization

The morphology of the P(VDF-TrFE)/$CoFe_2O_4$ printed layers were evaluated via scanning electron microscopy (SEM) with a Hitachi S-4800 set-up at 10 kV. Previouly,

samples were coated with a thin gold layer using a sputter coating (Polaron, model SC502).

The mechanical characterization was carried out in the tensile mode with a Shimadzu AGS-J 500N universal testing set-up. The samples were cut into rectangular geometry of 20 mm x 6 mm with a sample thickness of ≈50 μm. The Young´s modulus was calculated based on the evaluation of three replicas from the first linear slope of the stress-strain curves (in the range 0.5-1%). The standard deviation of the measurement was estimated to ±0.08 GPa.

The measurements of the capacity and dielectric loss tan δ were performed with an E4980A Precision LCR Meter in the measuring frequency range of 1 kHz to 1 MHz at an applied voltage of 0.5 V. In order to obtain a plane parallel condenser geometry, Au contacts with 5 mm diameter were deposited on both sides of the samples using a Polaron SC502 sputter coater (40 nm of gold thickness). The real part of the dielectric constant, ε´, was determined from the electrical capacity (C) taking into account the geometry of the sample (thickness (d) and electrode area (A)) (equation 1):

$$\varepsilon' = \frac{C \times d}{A} \qquad (1)$$

Magnetic hysteresis loops were measured at room temperature using an ADE 3473-70 Technologies vibrating sample magnetometer (VSM).

The poling of the samples was achieved, after an optimization procedure, (60 min of corona poling at 120 °C in a home-made chamber). In order to optimize the piezoelectric response, the electric field was kept applied when the samples were cooled to room temperature. The piezoelectric response (d_{33}) of the poled samples was obtained with a wide range d_{33}-meter (model 8000, APC Int. Ltd).

The ME response was obtained by measuring the transversal ME voltage coefficient (α_{33}) using the dynamic lock-in amplifier method[9]. A pair of Helmholtz coils was used to generate an AC magnetic field with amplitude of 1 Oe and frequency of ≈20 kHz (resonance of the composite) that is superimposed to a DC bias field driven by an electromagnet. Both fields are applied out of plane of the nanocomposite film and the generated voltage across the sample thickness is measured using a digital Lock-in amplifier (Stanford Research SR530). The ME voltage coefficient (α_{33}) was calculated from the measured voltage using equation 2:

$$\alpha_{33} = \frac{\Delta V}{H_{AC} \times t} \qquad (2)$$

where ΔV is the measured output voltage, H_{AC} is the amplitude of the AC magnetic field, and t is the thickness of the nanocomposite film.

3. Results and discussion

The morphology of the samples are shown in the SEM images presented in Figure 1. Both transversal (a) (obtained by cutting the samples after 1 minute immersion in LN_2) and surface (b) images reveal a fibrillar microstructure induced by the printing procedure.

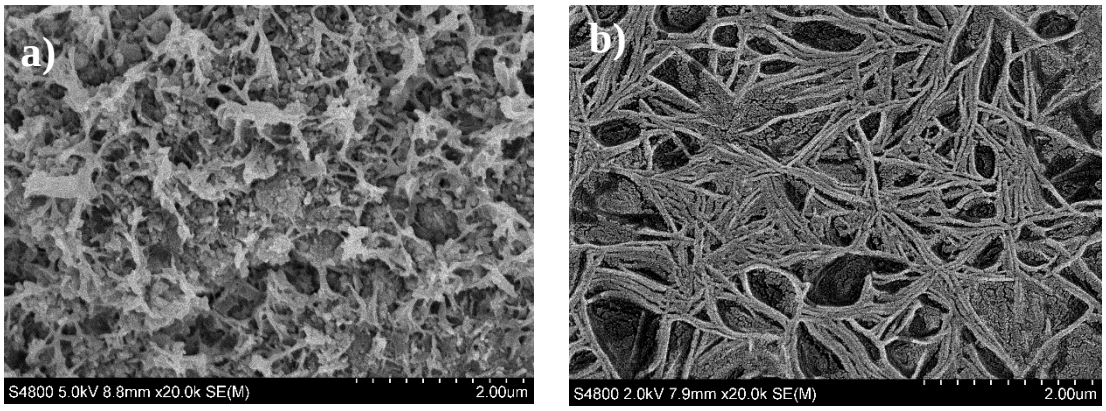

Figure 1. a) Transversal and b) surface. SEM images of the P(VDF-TrFE)/$CoFe_2O_4$ printed composites with 20 wt.% of ferrite content

Such fibrillar microstructure is typical for PVDF-TrFE, but, in the present case is reinforced by the mechanical energy of the gas flow followed by the polymer solidification in the form of fibers[10]. It is to notice that no filler agglomeration are observed, indicating a good dispersion of the magnetic nanoparticles. To verify if the obtained microstructure affects the mechanical properties of the spray-printed ME composites when compared with the ones obtained by bar coating, stress-strain measurements were performed (Figure 2).

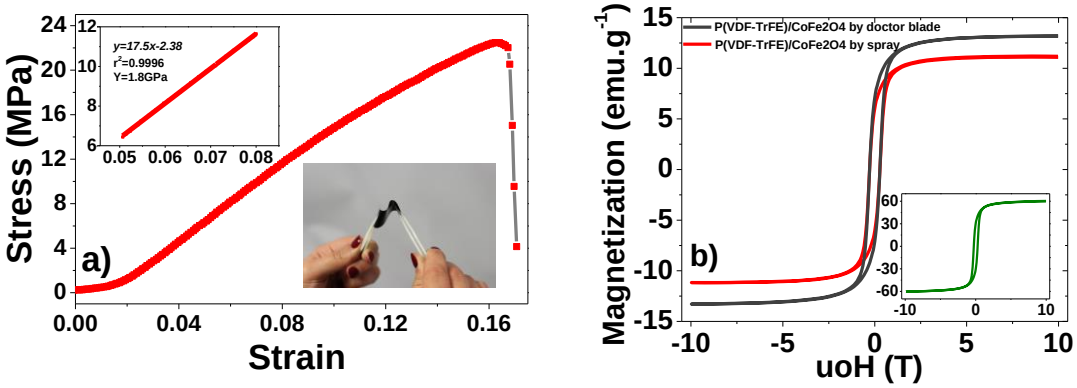

Figure 2. Characteristic stress-strain curve in the tensile mode of the P(VDF-TrFE)/ $CoFe_2O_4$ composite (the inset shows the linear fit to obtain the Young´s modulus and a photograph of the printed ME composite). b) Room-temperature magnetization as a function of the applied DC magnetic field. The inset shows the room-temperature magnetization of the $CoFe_2O_4$ nanoparticles.

The $CoFe_2O_4$/P(VDF-TrFE) samples shows a good mechanical stability (inset in figure 2 a) with the typical thermoplastic behaviour of pristine P(VDF-TrFE) polymer, with yielding strain at ≈2%. From the initial slope of the mechanical stress–strain curve, in-plane Young's modulus value, E, has been determined as ≈1.8 GPa. This value is the double of the pristine P(VDF-TrFE) polymer and other ME composites reported in the literature[11,12]. The increase in the Young's modulus and slight decrease in the value of elongation at the break point (from 3% to 2%) can be related with the enhancement in the crystalline zones, high levels of chain orientation and improved chain extension promoted by the elongation forces from the spray's gas flow[13,14].

The spray-printed P(VDF-TrFE)/ $CoFe_2O_4$ exhibits room-temperature ferromagnetism (Figure 2b) with a saturation magnetization of 11.2 $emu.g^{-1}$, 6.0 $emu.g^{-1}$ remanence and coercivity of 2050 Oe. values which are similar to the ones obtained for bar-coated P(VDF-TrFE)/$CoFe_2O_4$ composites, showing the lack of influence of the processing conditions on the nanofiller magnetic response.

Table I. Coercive field (HC), magnetic remanence, magnetic saturation and Cofe2O4 wt.% for P(VDF-TrFE)/ $CoFe_2O_4$ samples prepared by spray-printign and bar-coating, as well as for $CoFe_2O_4$ nanoparticles.

Material	H_c	M_r	M_s	$CoFe_2O_4$ wt.%
spray-printed $CoFe_2O_4$/P(VDF-TrFE)	2050	6	11	19
bar-coated $CoFe_2O_4$/P(VDF-TrFE)	2050	7	12	20
$CoFe_2O_4$ nanoparticles	2050	39	59	100

Magnetization measurements (Figure 2b) were also used to calculate the $CoFe_2O_4$ content on the spray-printed P(VDF-TrFE)/$CoFe_2O_4$ composite by the method proposed in[15], and compared with the value obtained in a similar composite obtained by bar-coating (Table 1). It is observed that the printing procedure does not affect the ferrite content in the composite.

Once the dielectric and piezoelectric properties of ME composites have a high impact on their multifunctional performance[11,16], the room-temperature dielectric response as a function of frequency and the room-temperature piezoelectric response as a function of the number of days after poling are presented in Figure 3.

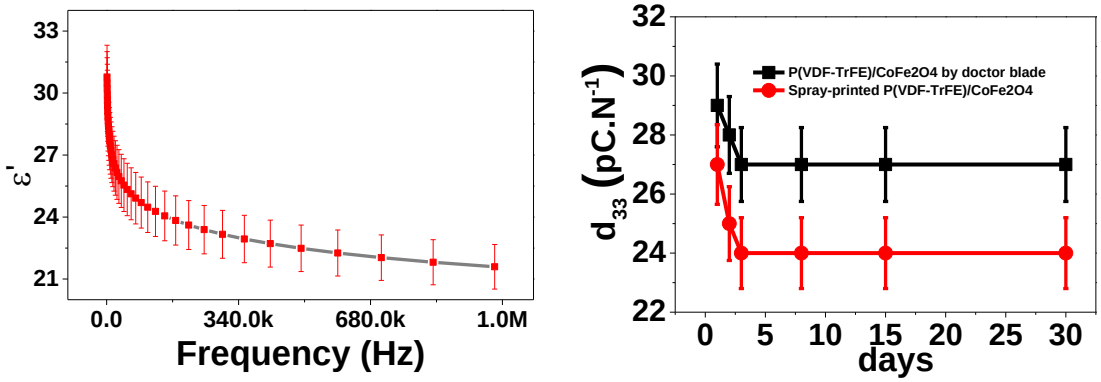

Figure 3. a) Frequency dependence of the real part of the permittivity (ε′) and b) room-temperature piezoelectric response of the ME P(VDF-TrFE)/$CoFe_2O_4$ sample.

Figure 3a shows that the real part of the dielectric response deceases rapidly with increasing frequency and decreases more moderately for frequencies above 10 kHz. This behaviour at the lower frequencies is explained by the Maxwell–Wagner type interfacial polarization, in agreement with Koop's phenomenological models[17]. Additionally, the inclusion of $CoFe_2O_4$ particles into the P(VDF-TrFE) matrix leads to a significant increase of the dielectric constant when compared with the dielectric response of the pristine polymer (from 10 to 31 at 10 kHz) explained by the interfacial polarization at the particle/polymer interfaces [18,19]. The result of the interfacial polarization at the particle/polymer interfaces is also noted in the difference between the piezoelectric response of the pristine polymer (24 $pC.N^{-1}$) and the one observed on the printed P(VDF-TrFE)/$CoFe_2O_4$ composite (27 $pC.N^{-1}$).

Such improved dielectric and piezoelectric responses anticipate a better ME coupling in the P(VDF-TrFE)/$CoFe_2O_4$ spray-printed composite (Figure 4).

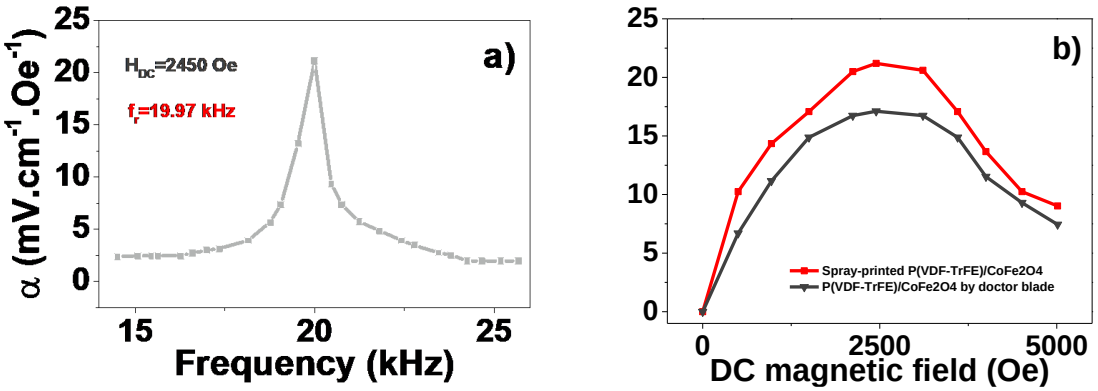

Figure 4. Room-temperature ME response of P(VDF-TrFE)/$CoFe_2O_4$ spray-printed composite as a function of the: a) frequency and; b) DC magnetic field. The ME coupling of the a similar P(VDF-TrFE)/$CoFe_2O_4$ composite obtained by the bar coating technique is also given for comparison.

The harmonic mode order, thickness, in-plane Young's modulus and density of the composites[20] placed the resonance of the P(VDF-TrFE)/$CoFe_2O_4$ spray-printed composite at 19.97 kHz. The DC ME characterization was performed at such frequency and it was verified a similar behaviour than for bar-coated composites, being observed that the ME coefficient increases with increasing DC magnetic field until a maximum of 21.2 mV·cm^{-1}·Oe^{-1} in the case of the spray-printed composite and 17.1 mV·cm^{-1}·Oe^{-1} in the case of the bar-coated-printed composite, both at an optimum magnetic field of 2450 Oe. Such behaviour is explained by the increase of the effective piezomagnetic coefficient until the optimum DC magnetic field is reached. With further increase in the DC magnetic field, a decrease in the induced voltage is observed for both composites resulting from the saturation of the magnetostriction coefficient[21]. The ≈4 mV·cm^{-1}·Oe^{-1} superior coefficient detected on the spray-printed samples can be explained by the higher dielectric coupling and superior piezoelectric response of the spray-printed composite when compared to the bar-coated composite[8].

4. Conclusions

A simple upscalable method for the preparation of ME materials based on spray-printing is reported. The resulting P(VDF-TrFE)/$CoFe_2O_4$, with 20 wt.% of ferrite content and a fibrillar structure exhibits improved dielectric and piezoelectric responses when compared to a composite with a similar composition but obtained by bar-coating, leading to an 21.2 mV·cm^{-1}·Oe^{-1} ME coupling coefficient at an optimum magnetic field of 2450 Oe suitable for sensor/actuator applications. The simple printing process, easy integration into devices and the possibility to be obtained over flexible and large areas validate the

developed ME material for applications such as printed electronics, sensors, actuators, and energy harvesters.

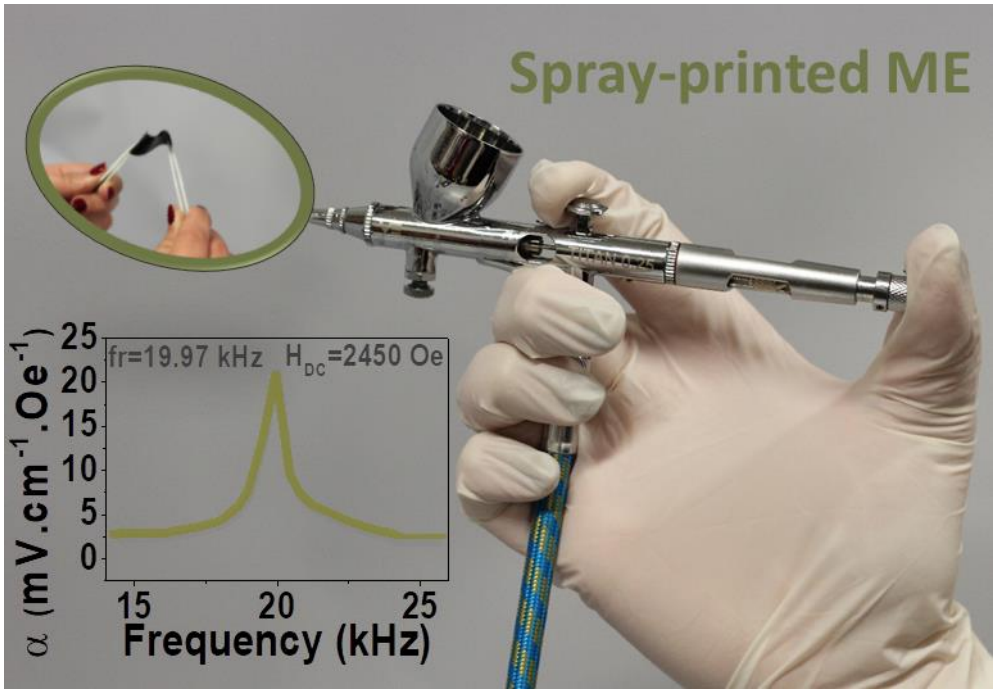

REFERENCES

(1) Oztan, C.; Ballikaya, S.; Ozgun, U.; Karkkainen, R.; Celik, E. *Applied Materials Today* **2019**, *15*, 77.

(2) Mendes-Felipe, C.; Oliveira, J.; Etxebarria, I.; Vilas-Vilela, J. L.; Lanceros-Mendez, S. *Advanced Materials Technologies* **2019**.

(3) Vaseem, M.; Ghaffar, F. A.; Farooqui, M. F.; Shamim, A. *Advanced Materials Technologies* **2018**, *3*.

(4) Oliveira, J.; Correia, V.; Castro, H.; Martins, P.; Lanceros-Mendez, S. *Additive Manufacturing* **2018**, *21*, 269.

(5) Zong, Y.; Zheng, T.; Martins, P.; Lanceros-Mendez, S.; Yue, Z.; Higgins, M. J. *Nature Communications* **2017**, *8*.

(6) Ferreira, A.; Lanceros-Mendez, S. *Composites Part B: Engineering* **2016**, *96*, 242.

(7) Martins, P.; Gonçalves, R.; Lopes, A. C.; Venkata Ramana, E.; Mendiratta, S. K.; Lanceros-Mendez, S. *Journal of Magnetism and Magnetic Materials* **2015**, *396*, 237.

(8) Martins, P.; Silva, M.; Lanceros-Mendez, S. *Nanoscale* **2015**, *7*, 9457.

(9) Martins, P.; Lasheras, A.; Gutierrez, J.; Barandiaran, J.; Orue, I.; Lanceros-Mendez, S. *Journal of Physics D: Applied Physics* **2011**, *44*, 495303.

(10) Lysak, I. A.; Malinovskaya, T. D.; Lysak, G. V.; Potekaev, A. I.; Kulagina, V. V.; Tazin, D. I. *Russian Physics Journal* **2017**, *59*, 1581.

(11) Brito-Pereira, R.; Ribeiro, C.; Lanceros-Mendez, S.; Martins, P. *Composites Part B: Engineering* **2017**, *120*, 97.

(12) Martins, P.; Moya, X.; Phillips, L. C.; Kar-Narayan, S.; Mathur, N. D.; Lanceros-Mendez, S. *Journal of Physics D: Applied Physics* **2011**, *44*.

(13) Moradi, R.; Karimi-Sabet, J.; Shariaty-Niassar, M.; Koochaki, M. A. *Polymers* **2015**, *7*, 1444.
(14) Yao, J.; Bastiaansen, C. W. M.; Peijs, T. *Fibers* **2014**, *2*, 158.
(15) Gonçalves, R.; Martins, P.; Correia, D. M.; Sencadas, V.; Vilas, J. L.; León, L. M.; Botelho, G.; Lanceros-Méndez, S. *RSC Advances* **2015**, *5*, 35852.
(16) Kisiel, A.; Konieczny, M.; Zabska, M. In *IOP Conference Series: Materials Science and Engineering*; 1 ed. 2016; Vol. 113.
(17) Gutiérrez, J.; Martins, P.; Gonçalves, R.; Sencadas, V.; Lasheras, A.; Lanceros-Mendez, S.; Barandiarán, J. M. *European Polymer Journal* **2015**, *69*, 224.
(18) Ummer, R. P.; Raneesh, R.; Thevenot, C.; Rouxel, D.; Thomas, S.; Kalarikkal, N. *RSC Advances* **2016**, *6*, 28069.
(19) Zhou, J. P.; Zhang, Y. X.; Liu, Q.; Liu, P. *Acta Materialia* **2014**, *76*, 355.
(20) Martins, P.; Silva, M.; Reis, S.; Pereira, N.; Amorín, H.; Lanceros-Mendez, S. *Polymers* **2017**, *9*, 62.
(21) Martins, P.; Kolen'Ko, Y. V.; Rivas, J.; Lanceros-Mendez, S. *ACS Applied Materials and Interfaces* **2015**, *7*, 15017.

ACKNOWLEDGMENTS

The authors thank the FCT- Fundação para a Ciência e Tecnologia- for financial support in the framework of the Strategic Funding UID/FIS/04650/2013 and under project PTDC/EEI-SII/5582/2014 P. Martins and J. Oliveira thanks the FCT for the FCT-SFRH/BPD/96227/2013 and SFRH/BD/98219/2013 grants respectively. Finally, the authors acknowledge funding by the Spanish Ministry of Economy and Competitiveness (MINECO) through the project MAT2016-76039-C4-3-R (AEI/FEDER, UE) and from the Basque Government Industry and Education Department under the ELKARTEK, HAZITEK and PIBA (PIBA-2018-06) programs, respectively.